

Article

Simple and Label-Free Detection of Carboxylesterase and Its Inhibitors Using a Liquid Crystal Droplet Sensing Platform

Duy-Khiem Nguyen  and Chang-Hyun Jang *

Department of Chemistry, Gachon University, Seongnam-daero 1342, Sujeong-gu, Seongnam-si 13120, Gyeonggi-do, Korea; khiem80@gachon.ac.kr

* Correspondence: chjang4u@gachon.ac.kr; Tel.: +82-31-750-8555

Abstract: In this study, we developed a liquid crystal (LC) droplet-based sensing platform for the detection of carboxylesterase (CES) and its inhibitors. The LC droplet patterns in contact with myristoylcholine chloride (Myr) exhibited dark cross appearances, corresponding to homeotropic anchoring of the LCs at the aqueous/LC interface. However, in the presence of CES, Myr was hydrolyzed; therefore, the optical images of the LC patterns changed to bright fan-shaped textures, corresponding to a planar orientation of LCs at the interface. In contrast, the presence of CES inhibitors, such as benzil, inhibits the hydrolysis of Myr; as a result, the LC patterns exhibit dark cross textures. This principle led to the development of an LC droplet-based sensing method with a detection limit of 2.8 U/L and 10 μ M, for CES detection and its inhibitor, respectively. The developed biosensor not only enables simple and label-free detection of CES but also shows high promise for the detection of CES inhibitors.

Keywords: carboxylesterase; liquid crystals (LC); myristoylcholine; LC droplet-based sensor; inhibitor



Citation: Nguyen, D.-K.; Jang, C.-H. Simple and Label-Free Detection of Carboxylesterase and Its Inhibitors Using a Liquid Crystal Droplet Sensing Platform. *Micromachines* **2022**, *13*, 490. <https://doi.org/10.3390/mi13030490>

Academic Editor: José Alberto Fracassi da Silva

Received: 4 March 2022

Accepted: 20 March 2022

Published: 21 March 2022

Publisher's Note: MDPI stays neutral with regard to jurisdictional claims in published maps and institutional affiliations.



Copyright: © 2022 by the authors. Licensee MDPI, Basel, Switzerland. This article is an open access article distributed under the terms and conditions of the Creative Commons Attribution (CC BY) license (<https://creativecommons.org/licenses/by/4.0/>).

1. Introduction

Liquid crystals (LCs) are promising materials for biosensing owing to their unique physical properties such as long-range orientational order, optical anisotropy, and molecular sensitivity [1,2]. Thus, LCs have been widely used to develop novel sensing systems for monitoring biochemical events [3,4]. LC-based sensing systems can transform chemical/biological events into optical responses that can be observed under a polarized light microscope (POM) [4,5]. Moreover, these sensing systems can operate in ambient environments without the need for molecular labels or electrical power [5–7]. Recently, LC-based sensors for monitoring various biochemical events have been developed and reported [5,7–10]. Among these, LC droplet-based sensors have been widely used to investigate enzymatic activity because the large surface-area-to-volume ratio of the LC droplets can increase the sensitivity of the detection [3,11]. The LC droplets were formed by simply dropping the solution of LC dissolved in organic solvents onto the surfaces of glass slides. The LC patterns exhibited bright fan-shaped appearances when in contact with non-surfactant solutions (e.g., deionized water), whereas dark cross textures were observed after introducing surfactant solutions [11,12].

Carboxylesterases (CESs) are an important class of enzymes that catalyze the hydrolysis of carboxylic esters and play a crucial role in the detoxification and metabolism of many drugs [13–15]. Moreover, the level of CES can serve as an indicator of hepatocellular carcinoma [16]. Thus, the accurate measurement of CESs is very helpful for better understanding their biological functions as well as for the early diagnosis of hepatocellular carcinoma.

To date, several detection methods, including fluorescence [14,15,17], chromatography [18], and luminescence [19,20], have been developed for CES detection. However, these methods have limitations including the need for complex instrumentation, labeling of samples, and long operating times. Recently, a simple and sensitive sensing system for CES

detection based on a surfactant-decorated LC/aqueous interface was reported [21]. However, some drawbacks need to be addressed. The copper grids used to prepare LC/aqueous interfaces are easily oxidized and deformed, which limits their reusability [11]. Moreover, when preparing LC thin films, excess LCs are removed from copper grid waste materials.

In this study, we developed a simple and sensitive LC droplet-based biosensor for CES detection. The structure diagram and principle of the developed sensor are illustrated in Figure 1. The LC droplet patterns were formed by spreading 1.5 μL of a heptane solution containing 2% (v/v) 5CB onto the OTS-modified glass slides after the evaporation of heptane. OTS with a hydrophobic tail was used to align the 5CB molecules at the glass/LC interface in a homeotropic orientation. Myristoylcholine (Myr, the substrate of the CES enzyme) was used as a cationic surfactant to induce homeotropic anchoring of LCs at the LC/aqueous interfaces, corresponding to the dark cross appearances of the LC droplets observed under POM (Figure 1B(a)). However, in the presence of CES, the optical images of the LC droplet patterns changed to bright fan-shaped textures owing to the enzymatic hydrolysis of Myr by CES (Figure 1B(b)). Moreover, the effect of the inhibitor on CES activity was investigated. This biosensor enables simple and fast detection of CES and its inhibitors with high selectivity.

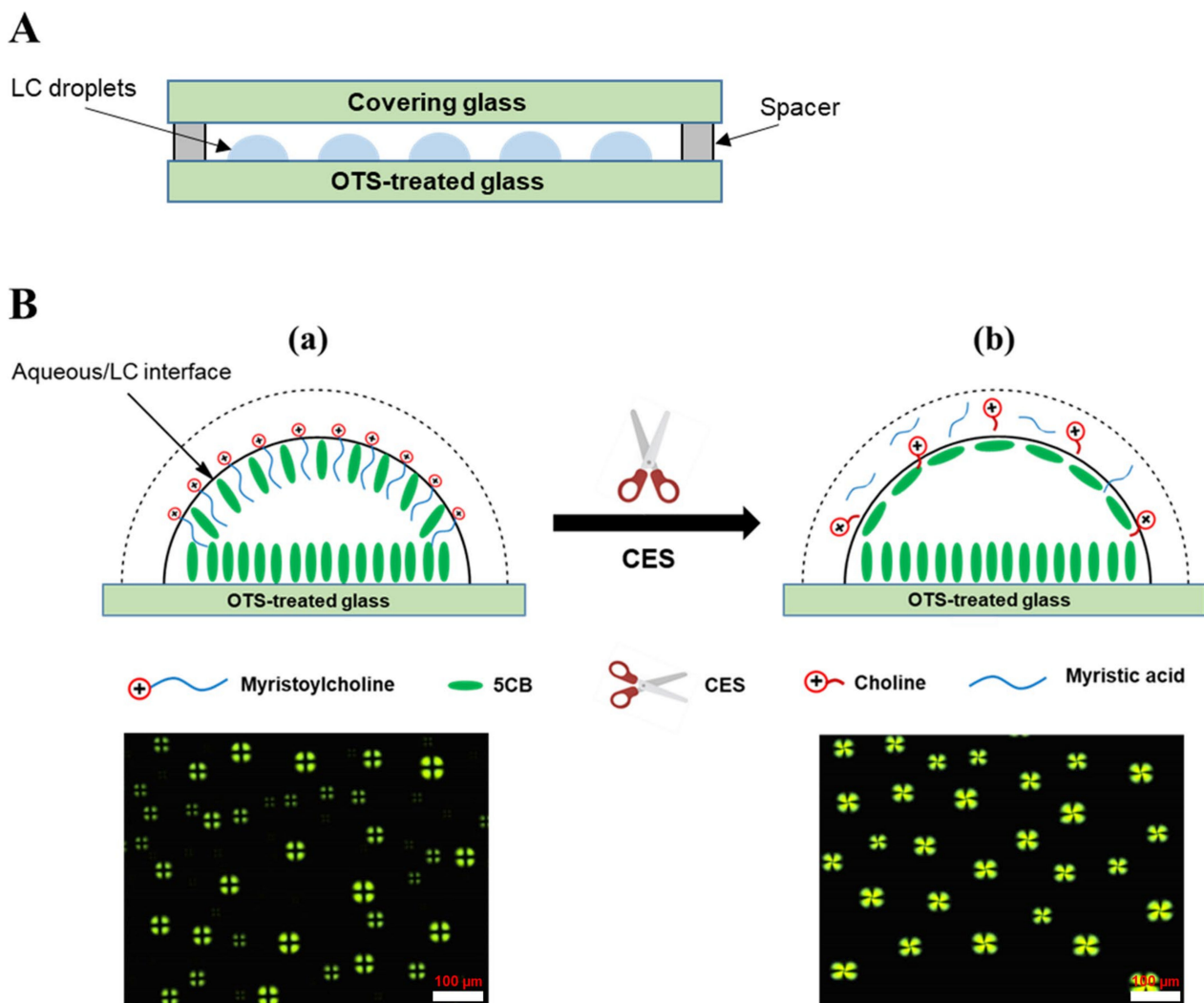


Figure 1. (A) Structure diagram of a liquid crystal (LC) cell; (B) Schematic illustration of the LC orientation transition at the aqueous/LC interface and the corresponding optical images: (a) after the addition of myristoylcholine chloride (Myr) solution; and (b) after introducing a mixture of Myr and carboxylesterase (CES).

2. Materials and Methods

2.1. Materials and Apparatus

The materials, reagents, and apparatus used in this study are listed in the Supplementary Materials section.

2.2. Preparation of Octyltrichlorosilane (OTS)-Modified Glass Slides

OTS-modified glass slides were prepared as previously described [22,23]. The details are provided in the Supplementary Materials section.

2.3. Preparation of LC Droplet Patterns and Fabrication of LC Cells

LC droplet patterns were prepared by dropping 1.5 μL of 5CB (2% (*v/v*) in heptane) onto the OTS-modified substrate. The solvent was evaporated at room temperature ($\sim 25^\circ\text{C}$) and LC droplet patterns were formed. Subsequently, approximately 100 μL of aqueous solution was transferred onto the LC droplets at 25°C . The LC cells were fabricated by pairing the covering glass slides and OTS-modified glass slides face to face (Figure 1A). Two small pieces of glass (26×0.5 mm, thickness = 1 mm) were used to produce a gap between two glass slides.

2.4. Preparation of the Aqueous Solution

All aqueous solutions were prepared in phosphate-buffered saline (PBS, 10 mM, pH = 7.4). During the CES detection assay, varying concentrations of CES were mixed with 10 μM Myr and incubated at 37°C for 30 min. For the enzyme inhibition assay, a mixture of CES (0.1 $\mu\text{g}/\text{mL}$) and benzil at various concentrations was pre-incubated at 37°C for 2 h. After the addition of 10 μM Myr, the mixtures were incubated at 37°C for 30 min. Subsequently, 100 μL of the incubated solution was added to the LC droplet at 25°C .

3. Results and Discussion

3.1. Optimization of the Myr Concentration

In our system, the LC droplet patterns were prepared by spreading 1.5 μL of an anhydrous heptane solution containing 2% (*v/v*) 5CB onto the OTS-modified glass slides. Here, Myr was used as a cationic surfactant to induce homeotropic anchoring of LCs at the LC/aqueous interfaces, corresponding to the dark cross appearances of the LC droplets observed under POM. Previous studies have demonstrated that the LC droplet patterns exhibited bright fan-shaped appearances when in contact with non-surfactant solutions (e.g., PBS solution), whereas dark cross textures were observed after introducing surfactant solutions [11,12]. Therefore, we first investigated the orientational behavior of 5CB at the aqueous/LC interface by comparing the optical responses of the LC droplets in contact with PBS and Myr solution. When the LC droplet pattern was immersed in PBS solution (pH = 7.4), we observed bright fan-shaped images coupled to the planar orientation of LCs at the interface (Figure 2a). However, the LCs adopted dark cross textures after the addition of 50 μM Myr solution (Figure 2b), corresponding to the homeotropic orientation of LCs at the aqueous/LC interface. This indicated that the addition of Myr altered the ordering of LCs at the interface from a planar to homeotropic orientation.

Next, we determined the minimum Myr concentration (C_{Myr}) to induce homeotropic orientation of the LCs by examining the optical response of LCs after reducing C_{Myr} . As shown in Figure 2, dark cross appearances were observed in LCs when $C_{\text{Myr}} \geq 10$ μM (Figure 2b–d), and bright fan-shaped images were observed when $C_{\text{Myr}} < 10$ μM (Figure 2e,f). Therefore, we determined that the critical C_{Myr} for inducing homeotropic orientation of LCs at the interface was approximately 10 μM .

3.2. Feasibility and Detection Limit of the LC Droplet-Based Biosensor for CES Detection

According to previous reports, CES can catalyze the hydrolysis of carboxylic acid esters into their corresponding acids and alcohols [21,24]. Thus, to verify the feasibility of the developed sensor, we studied the orientational transition of LCs at the interface

after introducing a mixture of Myr and CES. As shown in Figure 3a, bright fan-shaped images were observed after adding the mixture of Myr (10 μ M) and 100 mg/L CES to the LC droplet patterns, suggesting a planar orientation of LCs at the interface. This indicated that Myr was completely hydrolyzed by CES and demonstrated that CES activity could be monitored using the developed LC droplet biosensor.

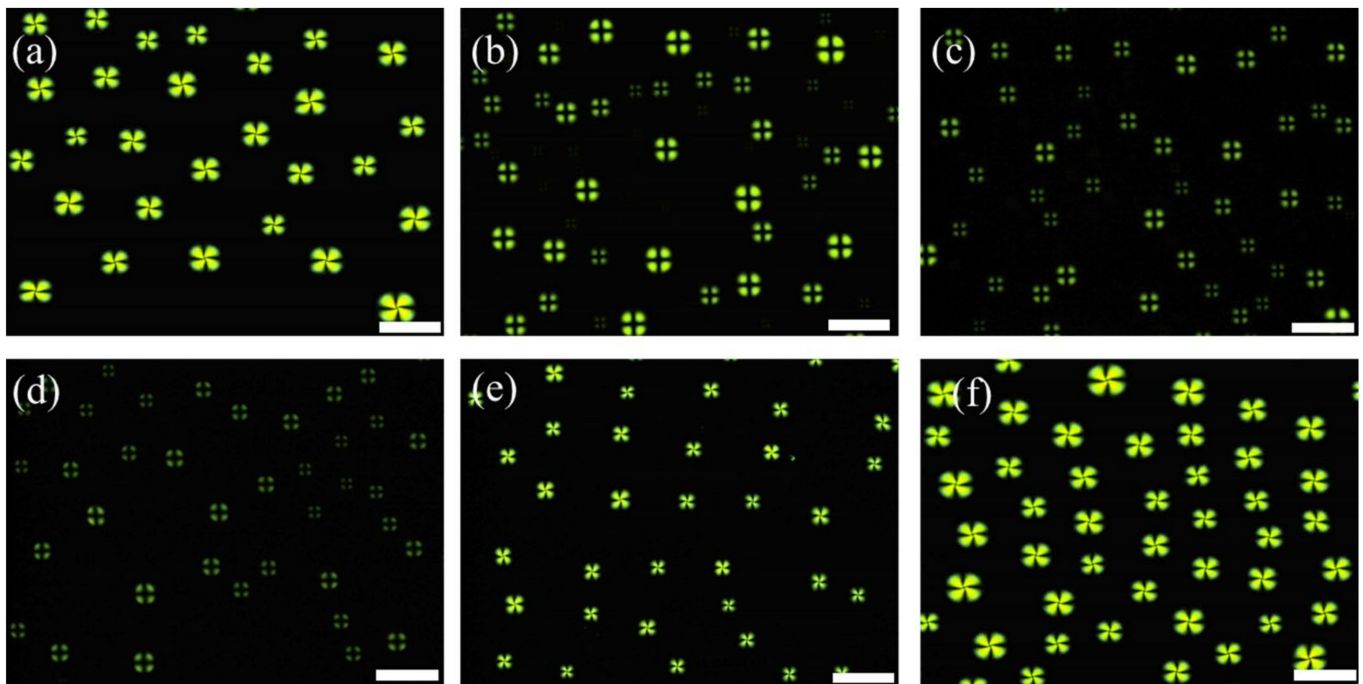


Figure 2. Optical images of liquid crystal (LC) droplets in contact with (a) PBS solution, and (b) 50 μ M, (c) 25 μ M, (d) 10 μ M, (e) 7.5 μ M, and (f) 5 μ M myristoylcholine chloride (Myr). Scale bar: 100 μ m.

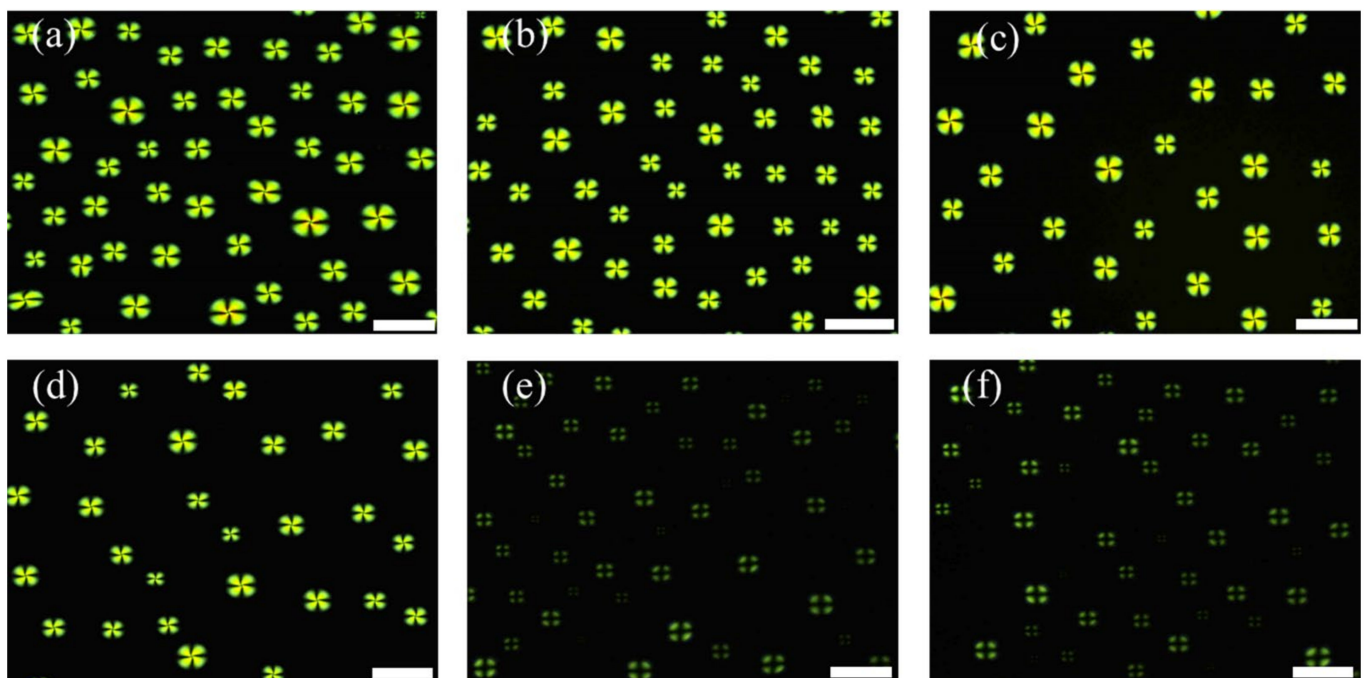


Figure 3. Optical images of liquid crystal (LC) droplets in contact with a pre-incubated mixture of 10 μ M myristoylcholine chloride (Myr) and varying concentrations of carboxylesterase: (a) 100 mg/L, (b) 10 mg/L, (c) 1 mg/L, (d) 0.1 mg/L, (e) 0.01 mg/L, and (f) 0.005 mg/L. Scale bar: 100 μ m.

Next, the limit of detection (LOD) for CES was determined by lowering the concentration of CES. The LC patterns showed bright fan-shaped images after incubating with pre-incubated mixtures containing 10 μM Myr and 10 mg/L, 1 mg/L, or 0.1 mg/L CES (Figure 3b–d). However, dark cross appearances were observed when the CES concentration was reduced to 0.01 mg/L or lower (Figure 3e,f), which was attributed to the incomplete hydrolysis of Myr by AChE. Therefore, we concluded that the LOD for CES using this LC droplet sensing system was 0.1 mg/L (2.8 U/L).

3.3. Specificity of the LC Droplet-Based Biosensor in CES Detection

The specificity of the developed sensor was also investigated. Various interfering substances, including urease, lipase, α -chymotrypsin, lysozyme, urea, glucose, and CaCl_2 , were used to test the specificity of the sensor. As shown in Figure 4, a bright fan-shaped texture was observed in the case of CES (Figure 4a), whereas dark cross appearances were obtained for other interfering substances (Figure 4b–h). These results demonstrate the high specificity of the proposed biosensor for CES detection.

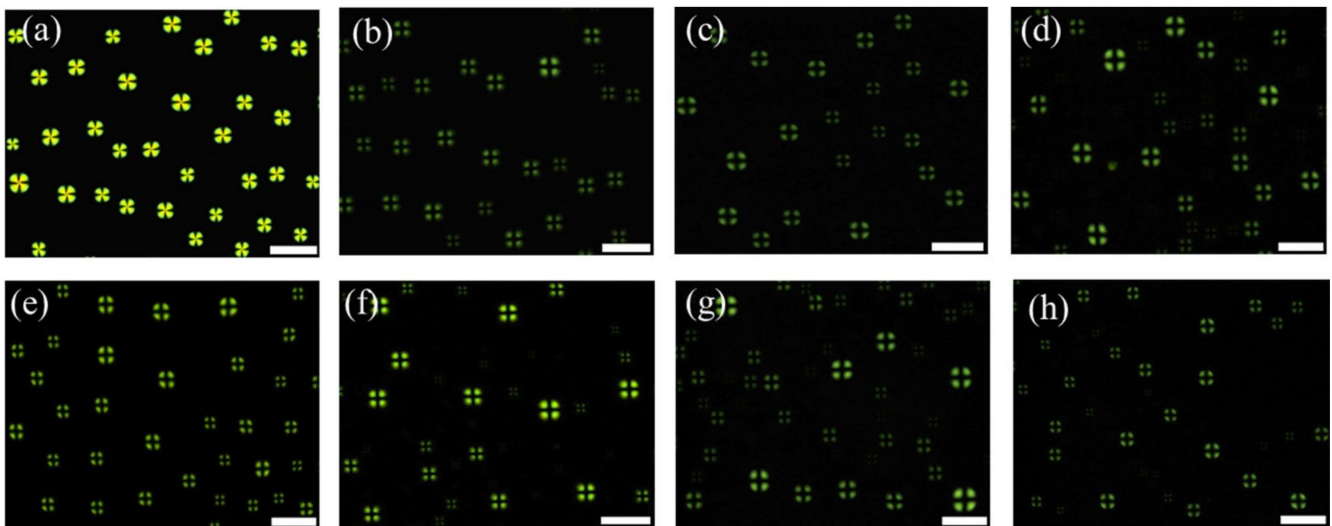


Figure 4. Optical images of liquid crystal (LC) droplets in contact with a pre-incubated mixture of 10 μM myristoylcholine chloride (Myr) and (a) 1 $\mu\text{g}/\text{mL}$ carboxylesterase (CES), (b) 100 $\mu\text{g}/\text{mL}$ urease, (c) 10 $\mu\text{g}/\text{mL}$ lipase, (d) 100 $\mu\text{g}/\text{mL}$ α -chymotrypsin, (e) 1 $\mu\text{g}/\text{mL}$ lysozyme, (f) 100 $\mu\text{g}/\text{mL}$ urea, (g) 100 $\mu\text{g}/\text{mL}$ glucose, and (h) 100 $\mu\text{g}/\text{mL}$ CaCl_2 . Scale bar: 100 μm .

It has been reported that benzil is a very potent CES inhibitor and exhibits selective inhibitory effects toward CES [25–27]. Therefore, to further confirm the specificity of the CES sensor, we investigated the optical images of LCs coupled with enzymatic hydrolysis of Myr with CES, which was pre-incubated with various benzil concentrations (C_{benzil}). Optical images of the LC droplets are presented in Figure 5. Dark cross appearances were obtained when $C_{\text{benzil}} \geq 10 \mu\text{M}$ (Figure 5a–c), indicating that CES activity was prevented by benzil. However, a bright fan-shaped texture was observed when the concentration of benzil was reduced to 1 μM (Figure 5d), suggesting that the concentration of benzil was too low to completely inhibit the activity of CES. These results further confirmed the high specificity of the LC droplet-based biosensor for CES detection. In addition, they also demonstrate the potential application of the LC droplet-based sensing system for the detection or screening of CES inhibitors.

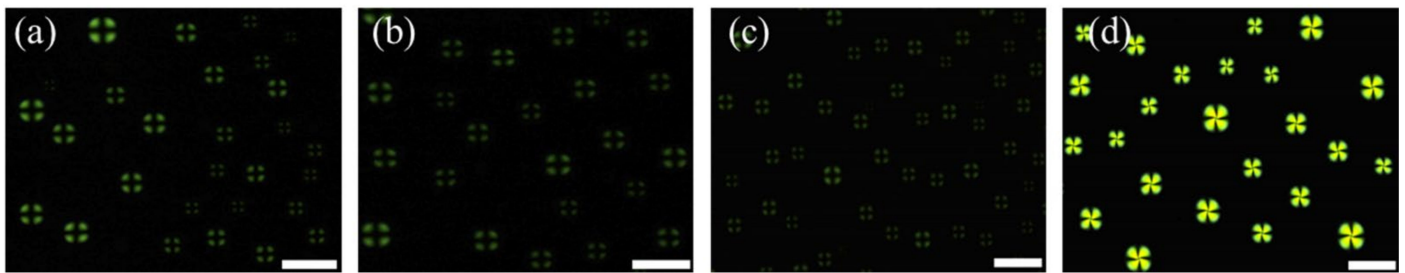


Figure 5. Optical images of liquid crystal (LC) droplets in contact with a mixture of 10 μ M myristoylcholine chloride (Myr) and 0.1 mg/L carboxylesterase (CES) pre-incubated with different concentrations of benzil: (a) 1 mM, (b) 100 μ M, (c) 10 μ M, and (d) 1 μ M. Scale bar: 100 μ m.

3.4. Detection of CES in Human Urine Samples

To evaluate the practicability of the developed biosensor, its ability to detect CES in human urine was examined. The human urine was collected from a healthy volunteer. The filtered human urine sample was diluted 10 times with PBS and then spiked with standard CES solution at a concentration of 5 mg/L. The spiked urine samples were analyzed using the developed biosensor. Human urine without the addition of CES was used as a control. The LC pattern displayed a dark cross in the control sample (Figure 6a), confirming there was no CES in the human urine. However, in the urine sample spiked with 5 mg/L CES, bright fan-shaped images were observed (Figure 6b), suggesting that the CES changed the orientation of LCs at the interface. These results prove the potential application of the developed sensing system for CES monitoring in real samples.

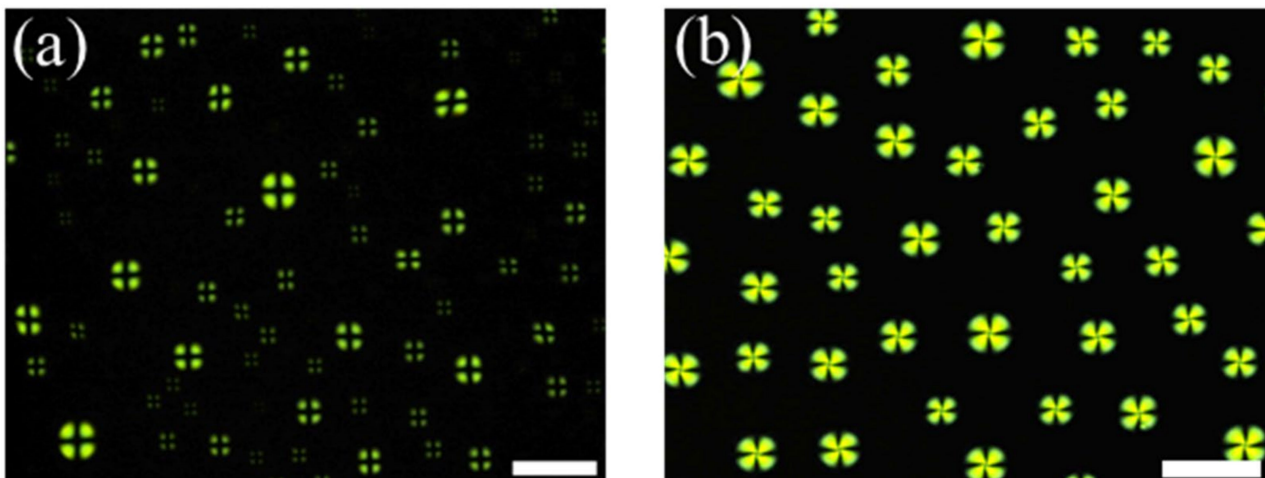


Figure 6. Optical images of liquid crystal (LC) droplets in contact with a mixture of 10 μ M myristoylcholine chloride (Myr) and (a) human urine (control), (b) human urine spiked with 5 mg/L carboxylesterase (CES). Scale bar: 100 μ m.

Before concluding, we compared the analytical characteristics of the developed LC droplet-based biosensor with other reported methods for CES detection such as spectroscopic, fluorescence, and bioluminescence. These detection methods are limited by several drawbacks such as the need for complex instrumentation, labeling of samples, and long operating times. In contrast, the proposed strategy offers a simple, rapid, label-free, and cost-effective method for the detection of CES with high selectivity. Using this method, a low detection limit of 0.1 mg/L (2.8 U/L) for CES was obtained, which is comparable to or lower than the LODs of other reported methods (Table 1).

Table 1. Comparison of the developed LC droplet-based strategy with other reported methods for carboxylesterase detection.

Methods	Linear Range	Detection Limit	Reference
Spectroscopic probe sensor	40–300 U/L	0.086 U/L	[14]
Near-infrared fluorescence probe	10–300 U/L	3.4 U/L	[15]
Bioluminescence sensor	0.01–6 mg/L	0.01 mg/L	[20]
Surfactant-doped LC-based sensor ^a	18–180 U/L	1 mg/L (18 U/L)	[21]
LC droplet-based biosensor	-	0.1 mg/L (2.8 U/L)	This study

^a LC, liquid crystal.

4. Conclusions

In summary, an LC droplet-based sensing platform was developed to monitor the enzymatic activity of CES, based on the optical responses of LC droplet patterns when in contact with surfactant or non-surfactant solutions. A dark cross appearance was obtained after the introduction of a cationic surfactant solution, Myr, onto the LC droplet patterns, whereas a bright fan-shaped optical image was observed after the addition of a pre-incubated mixture of Myr and CES, owing to the enzymatic hydrolysis of Myr by CES. However, the presence of CES inhibitors, such as benzil, inhibited CES activity resulting in a dark cross appearance. The proposed LC droplet-based biosensor exhibited high specificity toward CES with a low detection limit of 0.1 mg/L (2.8 U/L). In addition, the detection limit of the CES inhibitor was as low as 10 μ M. Moreover, the developed biosensor was successfully applied to detect CES in a real human urine sample. This LC droplet-based biosensor not only enables simple, rapid, and label-free detection of CES but also shows high potential for application in the detection or screening of CES inhibitors.

Supplementary Materials: Supporting information can be downloaded at: <https://www.mdpi.com/article/10.3390/mi13030490/s1>.

Author Contributions: Conceptualization, D.-K.N. and C.-H.J.; methodology, D.-K.N. and C.-H.J.; investigation, D.-K.N.; data curation, D.-K.N.; writing—original draft preparation, D.-K.N.; writing—review and editing, D.-K.N.; visualization, D.-K.N.; supervision, C.-H.J.; funding acquisition, C.-H.J. All authors have read and agreed to the published version of the manuscript.

Funding: This research was funded by Ministry of Education, grant number NRF-2019R1A2C1003862. The APC was funded by Duy-Khiem Nguyen.

Acknowledgments: This work was supported by the Basic Science Research Program of the National Research Foundation of Korea (NRF) funded by the Ministry of Education (NRF-2019R1A2C1003862).

Conflicts of Interest: The authors declare no conflict of interest.

References

- Hussain, A.; Pina, A.S.; Roque, A.C.A. Bio-recognition and detection using liquid crystals. *Biosens. Bioelectron.* **2009**, *25*, 1–8. [[CrossRef](#)] [[PubMed](#)]
- Hartono, D.; Xue, C.Y.; Yang, K.L.; Yung, L.Y.L. Decorating liquid crystal surfaces with proteins for real-time detection of specific protein–protein binding. *Adv. Funct. Mater.* **2009**, *19*, 3574–3579. [[CrossRef](#)]
- Wang, Y.; Hu, Q.; Tian, T.; Yu, L. Simple and sensitive detection of pesticides using the liquid crystal droplet patterns platform. *Sens. Actuators B Chem.* **2017**, *238*, 676–682. [[CrossRef](#)]
- Liao, S.; Qiao, Y.; Han, W.; Xie, Z.; Wu, Z.; Shen, G.; Yu, R. Acetylcholinesterase liquid crystal biosensor based on modulated growth of gold nanoparticles for amplified detection of acetylcholine and inhibitor. *Anal. Chem.* **2012**, *84*, 45–49. [[CrossRef](#)] [[PubMed](#)]
- Yang, X.; Li, H.; Zhao, X.; Liao, W.; Zhang, C.X.; Yang, Z. A novel, label-free liquid crystal biosensor for Parkinson’s disease related alpha-synuclein. *Chem. Commun.* **2020**, *56*, 5441. [[CrossRef](#)]
- Rouhbakhsh, Z.; Verdian, A.; Rajabzadeh, G. Design of a liquid crystal-based aptasensing platform for ultrasensitive detection of tetracycline. *Talanta* **2020**, *206*, 120246. [[CrossRef](#)] [[PubMed](#)]
- Wang, Y.; Hu, Q.; Guo, Y.; Yu, L. A cationic surfactant-decorated liquid crystal sensing platform for simple and sensitive detection of acetylcholinesterase and its inhibitor. *Biosens. Bioelectron.* **2015**, *72*, 25–30. [[CrossRef](#)]

8. Wu, W.; Wang, W.; Qi, L.; Wang, Q.; Yu, L.; Lin, J.M.; Hu, Q. Screening of Xanthine Oxidase Inhibitors by Liquid Crystal-Based Assay Assisted with Enzyme Catalysis-Induced Aptamer Release. *Anal. Chem.* **2021**, *93*, 6151–6157. [[CrossRef](#)] [[PubMed](#)]
9. McUmber, A.C.; Noonan, P.S.; Schwartz, D.K. Surfactant–DNA interactions at the liquid crystal–aqueous interface. *Soft Matter* **2012**, *8*, 4335–4342. [[CrossRef](#)]
10. Munir, S.; Park, S.Y. Liquid crystal-based DNA biosensor for myricetin detection. *Sens. Actuators B Chem.* **2016**, *233*, 559–565. [[CrossRef](#)]
11. Liu, D.; Jang, C.H. A new strategy for imaging urease activity using liquid crystal droplet patterns formed on solid surfaces. *Sens. Actuators B Chem.* **2014**, *193*, 770–773. [[CrossRef](#)]
12. Wei, Y.; Jang, C.H. Optical imaging of cholyglycine by using liquid crystal droplet patterns on solid surfaces. *J. Mater. Sci.* **2016**, *51*, 2033–2040. [[CrossRef](#)]
13. Di, L. The impact of carboxylesterases in drug metabolism and pharmacokinetics. *Curr. Drug Metab.* **2019**, *20*, 91–102. [[CrossRef](#)] [[PubMed](#)]
14. Zhang, Y.; Chen, W.; Feng, D.; Shi, W.; Li, X.; Ma, H. A spectroscopic off-on probe for simple and sensitive detection of carboxylesterase activity and its application to cell imaging. *Analyst* **2012**, *137*, 716. [[CrossRef](#)]
15. Li, W.; Zhai, C.; Wang, S.; Huang, W.; Liu, Y.; Li, Z. Detection of carboxylesterase by a novel hydrosoluble near-infrared fluorescence probe. *RSC Adv.* **2019**, *9*, 40689. [[CrossRef](#)]
16. Na, K.; Lee, E.Y.; Lee, H.J.; Kim, K.Y.; Lee, H.; Jeong, S.K.; Jeong, A.S.; Cho, S.Y.; Kim, S.A.; Song, S.Y.; et al. Human plasma carboxylesterase 1, a novel serologic biomarker candidate for hepatocellular carcinoma. *Proteomics* **2009**, *9*, 3989–3999. [[CrossRef](#)]
17. Dai, J.; Zhao, Y.; Hou, Y.; Zhong, G.; Gao, R.; Wu, J.; Shen, B.; Zhang, X. Detection of carboxylesterase 1 and carbamates with a novel fluorescent protein chromophore based probe. *Dyes Pigment.* **2021**, *192*, 109444. [[CrossRef](#)]
18. Koitka, M.; Hochel, J.; Obst, D.; Rottmann, A.; Gieschen, H.; Borchert, H.H. Determination of rat serum esterase activities by an HPLC method using S-acetylthiocholine iodide and p-nitrophenyl acetate. *Anal. Biochem.* **2008**, *381*, 113–122. [[CrossRef](#)] [[PubMed](#)]
19. Steinkamp, T.; Schweppe, F.; Krebs, B.; Karst, U. A tripod ligand as new sensitiser for the enzyme amplified lanthanide luminescence determination of esterase. *Analyst* **2003**, *128*, 29. [[CrossRef](#)]
20. Wang, D.D.; Jin, Q.; Zou, L.W.; Hou, J.; Lv, X.; Lei, W.; Cheng, H.L.; Ge, G.B.; Yang, L. A bioluminescent sensor for highly selective and sensitive detection of human carboxylesterase 1 in complex biological samples. *Chem. Commun.* **2016**, *52*, 3183–3186. [[CrossRef](#)]
21. Zhou, L.; Kang, Q.; Fang, M.; Yu, L. Label-free, rapid, and sensitive detection of carboxylesterase using surfactant-doped liquid crystal sensor. *J. Mol. Liq.* **2019**, *296*, 111921. [[CrossRef](#)]
22. Brake, J.M.; Abbott, N.L. An Experimental System for Imaging the Reversible Adsorption of Amphiphiles at Aqueous-Liquid Crystal Interfaces. *Langmuir* **2002**, *18*, 6101–6109. [[CrossRef](#)]
23. Duong, T.D.S.; Jang, C.H. A label-free liquid crystal droplet-based sensor used to detect lead ions using single-stranded DNAzyme. *Colloid Surface A* **2020**, *604*, 125304. [[CrossRef](#)]
24. Jin, Q.; Feng, L.; Wang, D.D.; Wu, J.J.; Hou, J.; Dai, Z.R.; Sun, S.G.; Wang, J.Y.; Ge, G.B.; Cui, J.N.; et al. A highly selective near-infrared fluorescent probe for carboxylesterase 2 and its bioimaging applications in living cells and animals. *Biosens. Bioelectron.* **2016**, *83*, 193–199. [[CrossRef](#)]
25. Zou, L.W.; Jin, Q.; Wang, D.D.; Qian, Q.K.; Hao, D.C.; Ge, G.B.; Yang, L. Carboxylesterase inhibitors: An update. *Curr. Med. Chem.* **2018**, *25*, 1627–1649. [[CrossRef](#)]
26. Wadkins, R.M.; Hyatt, J.L.; Wei, X.; Yoon, K.J.P.; Wierdl, M.; Edwards, C.C.; Morton, C.L.; Obenauer, J.C.; Damodaran, K.; Beroza, P.; et al. Identification and characterization of novel benzil (diphenylethane-1,2-dione) analogues as inhibitors of mammalian carboxylesterases. *J. Med. Chem.* **2005**, *48*, 2906–2915. [[CrossRef](#)] [[PubMed](#)]
27. Fleming, C.D.; Bencharit, S.; Edwards, C.C.; Hyatt, J.L.; Tsurkan, L.; Bai, F.; Fraga, C.; Morton, C.L.; Howard-Williams, E.L.; Potter, P.M.; et al. Structural Insights into Drug Processing by Human Carboxylesterase 1: Tamoxifen, Mevastatin, and Inhibition by Benzil. *J. Mol. Biol.* **2005**, *352*, 165–177. [[CrossRef](#)]